Bull. Mater. Sci., Vol. 39, No. 5, September 2016, pp. 1157–1163. © Indian Academy of Sciences.
DOI 10.1007/s12034-016-1261-4

Synthesis and luminescence properties of Tb^{3+}-doped $LiMgPO_4$ phosphor

C B PALAN[1,*], N S BAJAJ[2], A SONI[3] and S K OMANWAR[1]

[1]Department of Physics, Sant Gadge Baba Amravati University, Amravati 444 602, India
[2]Department of Physics, Toshniwal ACS College, Sengaon, Hingoli 431 542, India
[3]Radiological Physics and Advisory Division, Bhabha Atomic Research Centre, Mumbai 400 094, India

MS received 16 September 2015; accepted 16 March 2016

Abstract. **Polycrystalline sample $LiMg_{(1-x)}PO_4{:}xTb^{3+}$ ($x = 0.001, 0.002, 0.005, 0.01, 0.02$) phosphor was synthesized via modified solid state method (MSSM). The prepared sample was characterized through XRD pattern (X-ray diffraction) and SEM (scanning electron microscope). Additionally, photoluminescence (PL), optically stimulated luminescence (OSL), thermoluminescence (TL) and other dosimetric properties including dose linearity, reusability and fading were studied. In OSL mode, sensitivity of prepared phosphor was found to be 2.7 times that of $LiMgPO_4{:}Tb^{3+}$, B (BARC) phosphor and 4.3 times that of α-Al_2O_3:C (BARC) phosphor. The TL glow consists of overlapping peaks in temperature range of 50–400°C and first peak (P_1) was observed at 150°C, second peak (P_2) at 238°C, third peak (P_3) at 291°C and fourth peak (P_4) at 356°C. The TL sensitivity of second peak (P_2) of $LiMgPO_4{:}Tb^{3+}$ phosphor was compared with α-Al_2O_3:C (BARC) phosphor and found to be 100 times that of the α-Al_2O_3:C (BARC) phosphor. The minimum detectable dose (MDD) was found to be 5.6 μGy. Moreover, photoionization cross-sections, linearity, reusability, fading and kinetic parameters were calculated. Also, photoluminescence spectra of $LiMgPO_4{:}Tb^{3+}$ shows characteristic green–yellow emission exciting at 224 nm UV source.**

Keywords. **$LiMgPO_4{:}Tb^{3+}$ phosphor; TLD-500; modified solid state method; radiation dosimetry.**

1. Introduction

Optically stimulated luminescence (OSL) is a well-established technique in personal and medical dosimetry, particularly in conjunction with Al_2O_3:C OSL detectors [1]. The OSL technique provides fast readouts, re-evaluation of dose with same dosimeter and simple analysis as compared with thermoluminescence (TL) [2]. The technique was first suggested for personal dosimetry in 1950s. Further, it was spurred by introduction of a method of equivalent dose determination in this area by Huntley *et al* [3,4].

From last two decades, various materials have been suggested by the numorous researchers throughout the world. Out of those, few were exposed to the commercial scene. In this range of materials, the phosphate-based materials doped with trivalent rare earth ions (RE^{3+}) have attracted extensive attention because of their remarkable luminescence properties and useful applications. Moreover, orthophosphates have attracted intense attention particularly in OSL.

Till date, many researchers worked on the series of phosphate-based phosphors, mainly, $ABPO_4$ structure, where A is a monovalent cation (Li^+, Na^+, K^+, Rb^+, Cs^+) and B is a divalent cation (Mg^{2+}, Ca^{2+}, Sr^{2+}, Ba^{2+}) due to their large bandgap along with the high absorption of PO_4^{3-} in UV region, moderate phonon energy, high thermal and chemical stability and exceptional optical damage threshold [5–7]. Recently, $LiMgPO_4{:}Tb^{3+}$, B, $LiMgPO_4{:}Tb^{3+}$, Sm, B, $LiBaPO_4{:}Tb^{3+}$, $LiCaPO_4$:Eu, and Li_3PO_4:M (M = Tb, Cu) have been reported as a new phosphor materials for potential applications in radiation dosimetry [8–12].

The phosphor $LiMgPO_4$ has become a material of choice for OSL dosimetry during last five years because of their excellent dosimetric properties such as high sensitivity, reusability, stability and effective atomic number (Z_{eff} = 11.44) equivalent to that of α-Al_2O_3:C (Z_{eff} = 11.28) phosphor. These qualities enforced the researcher to synthesize this phosphor with different methods with effects of dopant and co-dopants too. Dhabekar *et al* [8] report $LiMgPO_4{:}Tb^{3+}$, B phosphor using solid state reaction. Similarly, Gai *et al* [9] developed the same phosphor using some other dopant and co-dopants.

In this work, we have investigated the TL and OSL properties of $LiMgPO_4{:}Tb^{3+}$ phosphor was synthesized via modified solid state method (MSSM). The MSSM is of low-cost and operate the materials at low temperature without specific atmosphere for synthesis.

To our knowledge, TL and OSL properties of Tb-doped $LiMgPO_4$ phosphor under beta irradiation rarely reported in the literature. In the present report, the preliminary results of TL and OSL properties of $LiMgPO_4{:}Tb^{3+}$ phosphor were presented.

*Author for correspondence (chetanpalan27@yahoo.in)

2. Experimental

The $LiMg_{(1-x)}PO_4:xTb^{3+}$ (x = 0.001, 0.002, 0.005, 0.01, 0.02) phosphor was synthesized via modified solid state method (MSSM). High purity starting materials, lithium nitrate $Li(NO_3)_3$, magnesium nitrate $Mg(NO_3)_2{\cdot}6H_2O$, ammonium dihydrogen phosphate $NH_4H_2PO_4$ and terbium nitrate (Tb_4O_7 + HNO_3) were used in the synthesis. The details of molar ratio of constituents used for phosphor synthesis is given in table 1. The starting materials were taken in a proper stoichiometric ratio mixed in china basin and adding small amounts of acetone, a clear solution was obtained. This mixture was heated on hot plate under 50°C for 30 min and then sample was placed in muffal furnace with the instalment of 100°C for 1 h, 200°C for 2 h, 400°C for 3 h, 800°C for 4 h and 1000°C for 1 h between two intermediate regrindings and sample was suddenly quenched at room temperature.

The phase purity of $LiMg_{(1-x)}PO_4:xTb^{3+}$ phosphor was checked by X-ray powder diffraction (PXRD) using a Rigaku miniflex II diffractometer with CuKα (l = 1.5405 Å) operated at 5 kV. The data were collected in a 2θ range from 10 to 70°. The structural and morphological characteristics i.e., particle size and shape of particle sample were studied using a scanning electronic microscope (SEM). In this study, sample in powder form (50–100 μm) was placed directly into a SEM for imaging. The measurement was performed on Philips XL 30 system at North Maharashtra University, Jalgaon. Irradiations of all the samples were performed at room temperature using a calibrated $^{90}Sr/^{90}Y$ beta source in-housed in RISO TL/OSL Reader (DA-15 Model). The activity of the source was 40 mCi and the dose rate was 20 mGy s^{-1}. All TL/OSL measurements were carried out using an automatic Risø TL/OSL-DA-15 reader system which can accommodate up to 48 discs. Blue LEDs emitting at 470 nm (FWHM = 20 nm) are arranged in four clusters each containing seven individual LEDs. The fading response of prepared $LiMgPO_4$:Tb phosphor was measured at Department of Physics, S.G.B. Amravati University by using PC CONTROLLED TL/OSL-1008 reader [13]. The PL and PL excitation (PLE) spectra were measured on (Hitachi F-7000) fluorescence spectrophotometer with a 450 W xenon lamp, in the range of 200–700 nm, with spectral slit width of 1 nm and PMT voltage 700 V at room temperature.

Table 1. Molar ratio of ingredients used for material preparation and corresponding chemical reaction.

Product	Corresponding reaction with balanced molar ratios of precursors
$LiMg_{(1-x)}PO_4:xTb^{3+}$	$Li(NO)_3 + Mg_{(1-x)}(NO_3)_2{\cdot}6H_2O + NH_4H_2PO_4 + xTb_4O_7$ {in stock solution form 1 g = 100 ml} = $LiMg_{(1-x)}PO_4:xTb^{3+}$ + gaseous products (H_2O, NH_3 and NO_2), (x = 0.001, 0.002, 0.005, 0.01, 0.02)

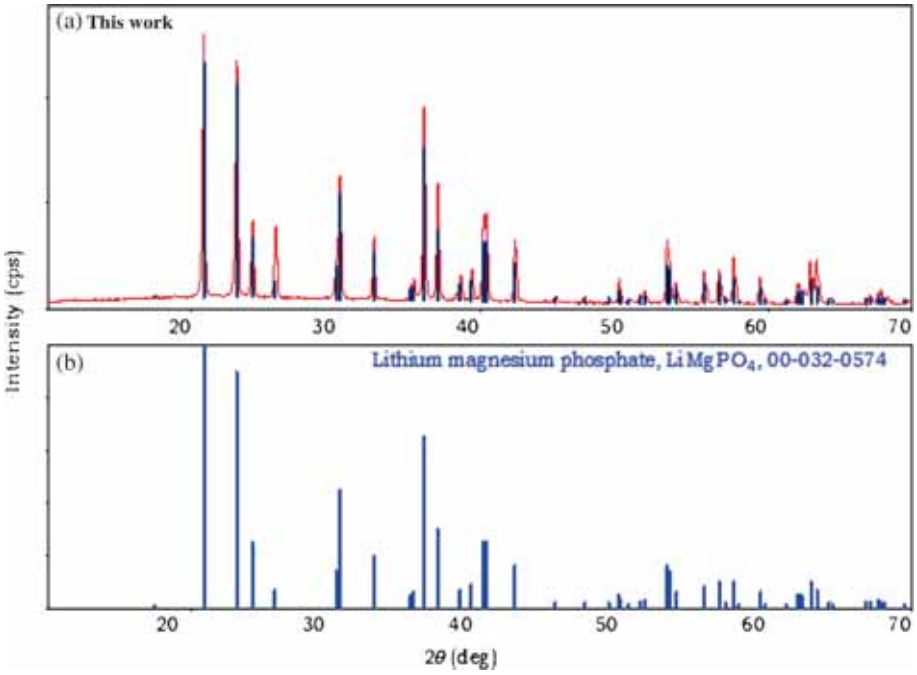

Figure 1. (**a**) X-ray diffraction patterns of $LiMgPO_4:Tb^{3+}$ phosphor and (**b**) standard data ICDD file.

3. Results and discussion

3.1 *XRD pattern*

The crystal phase formation of the sample was checked by using powder X-ray diffraction (XRD) technique. The XRD pattern of $LiMgPO_4:Tb^{3+}$ is shown in figure 1. The experimental pattern of $LiMgPO_4:Tb^{3+}$ was compared with the ICDD (International Centre for Diffraction Data) pattern with PDF card no. 00-032 0574. By a comparison between them, the position and intensity of the main peaks are the same. No impurity lines were observed, indicating the only crystalline product in sample. The $LiMgPO_4$ phosphor was orthorhombic, with the space group *Pnma* with *a* about twice than *b* and *c* cell constants.

3.2 *Surface morphology*

Figure 2 shows the SEM image of $LiMgPO_4:Tb^{3+}$ phosphor. From figure 2, it is observed that the microstructure of the phosphor consist of irregular grains with heavy agglomerate. The average size of as-synthesized phosphor particles were about 1–10 μm.

3.3 *Tb^{3+} luminescence*

3.3a *Concentration of Tb^{3+} activator*: Figure 3 represents the continuous wave OSL (CW-OSL) curves of $LiMgPO_4$ phosphor-doped with different concentrations of Tb^{3+}. During this study, all the samples with different concentrations were exposed to 20 mGy of β-ray simultaneously and weight of all the samples was same. However, concentrations of Tb^{3+} varies from 0.001 to 0.02 moles. From figure 3, it was observed that 0.01 mol was the optimum concentration for the prepared phosphor. The luminescence intensity was observed to be decreased when the concentration of Tb^{3+} ions were increased beyond this optimum value, due to well known phenomenon of concentration quenching [14].

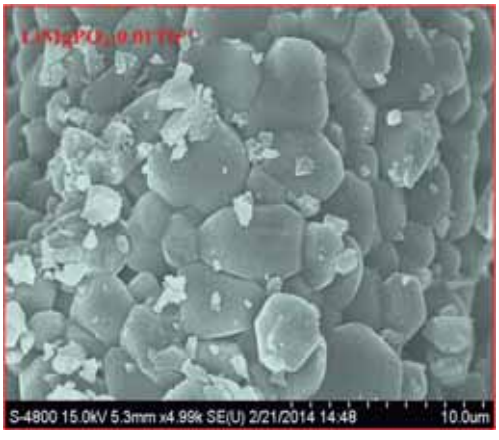

Figure 2. SEM pattern of $LiMgPO_4:Tb^{3+}$ phosphor.

3.3b *Comparison of sensitivity with commercially available OSLD materials*: Figure 4 represents third order exponentially decay curve of $LiMgPO_{4:0.01}Tb^{3+}$ phosphor for 20 mGy dose. Third order exponentially decay curve shows the presence of three components and having photoionization cross-sections of 0.56×10^{-17}, 4.14×10^{-17} and 8.84×10^{-17} cm^2, respectively, calculated parameters are given in table 2.

Figure 5 represents the comparison of $LiMgPO_4:Tb^{3+}$ phosphor with the α-Al_2O_3:C (BARC) and $LiMgPO_4:Tb^{3+}$, B (BARC) phosphor. From figure 5, it is observed that sensitivity of $LiMgPO_{4:0.01}Tb^{3+}$ phosphor was 2.7 times that of $LiMgPO_4:Tb^{3+}$, B (BARC) and 4.3 times that of α-Al_2O_3:C (BARC) phosphor.

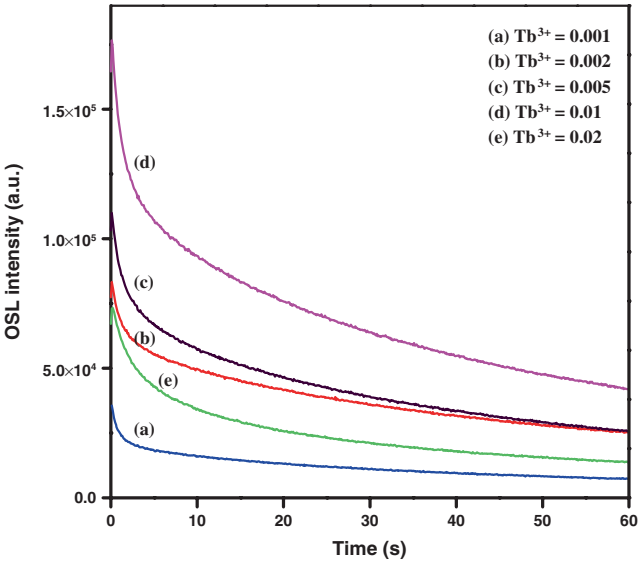

Figure 3. OSL response of $LiMgPO_4$ phosphor with different concentrations of Tb^{3+} ions.

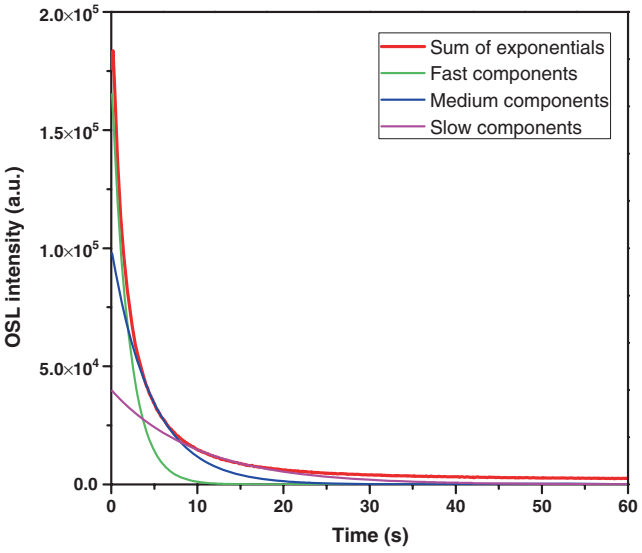

Figure 4. Third order exponential decay curve of $LiMgPO_4:Tb^{3+}$ phosphor.

Table 2. CW-OSL parameters of $LiMgPO_4:Tb^{3+}$ phosphor.

CW-OSL component	Coefficient A	Decay constant, τ (s)	Photo-ionization cross-section, σ (cm^2)	R^2
Fast	173567	2	0.56×10^{-17}	0.99917
Medium	100000	4.68	4.14×10^{-17}	
Slow	40000	10	8.84×10^{-17}	

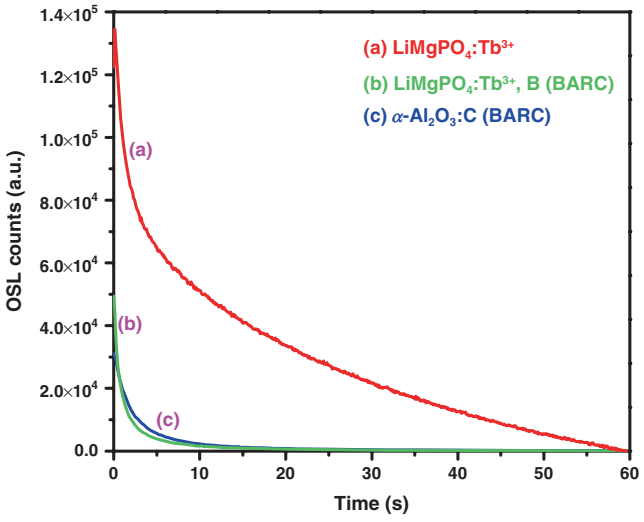

Figure 5. OSL response of (**a**) $LiMgPO_4:Tb^{3+}$ phosphor compared with (**b**) $LiMgPO_4:Tb^{3+}$, B phosphor and (**c**) α-Al_2O_3:C phosphor.

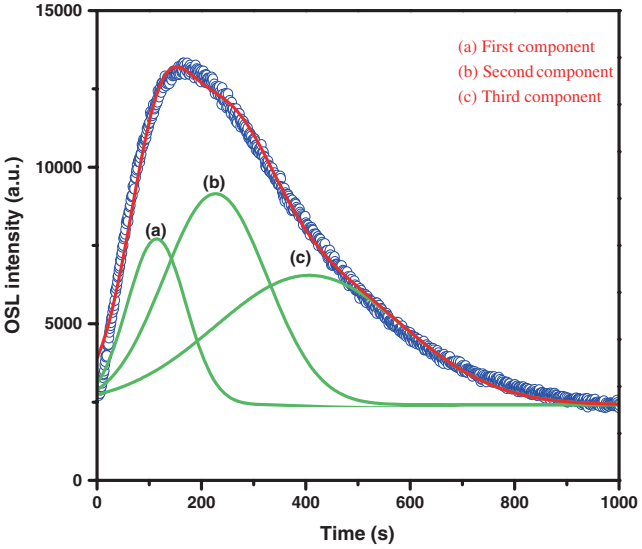

Figure 6. LM-OSL response of $LiMgPO_4:Tb^{3+}$ phosphor.

3.3c *Linear modulation OSL (LM-OSL)*: In OSL dosimetry, CW-OSL and pulsed OSL (POSL) are common read out modes. These modes control the high degree of stimulation intensity. Bulur *et al* [15] proposed recording the OSL curves using stimulation with an intensity that increases linearly with time, instead of remaining constant, an approach later referred to as linear modulation OSL (LM-OSL). Figure 6 represents LM-OSL curve of $LiMgPO_4:Tb^{3+}$ phosphor under β irradiation. One of the advantage of LM-OSL mode is components appear as superimposed peaks and these peaks deconvoluted. Three LM-OSL components were recognized in the OSL curve similar to component present in CW-OSL mode. Kumar *et al* [16] reported criteria for first order kinetics. The calculated kinetic parameters were given in table 3. From values of these kinetics parameters, LM-OSL curved obey first order kinetics.

3.3d *Reusability*: Reusability is one of the most important properties of dosimetric phosphor. This study was carried out by exposing the discs of $LiMgPO_4:Tb^{3+}$ phosphor under 20 mGy dose of β irradiation. Its OSL was recorded for 60 s after which again it was measured for 100 s, so that the discs were bleached completely. Ten such cycles were carried out as shown in figure 7. The studies show that the phosphor can be reused for 10 cycles without change in the OSL output.

3.3e *MDD*: The minimum detectable dose (MDD) of a phosphor depends on the standard deviation of the background signal which affects the signal to noise ratio [17]. MDD was found to be 5.6 μGy corresponding to 3σ of the background.

3.3f *Dose response*: Figure 8 shows the dose response of $LiMgPO_4:Tb^{3+}$ phosphor over the dose range of 0.04–10 Gy of β radiations. Additional filter was inserted to adjust the high sensitivity of this phosphor within measurable range of the instrument. Each data point represents the average of two different measurements. A linear dose response up to 10 Gy with linear correlation coefficient was found to be 0.9827.

3.3g *Fading*: Fading was studied by exposing the powder pouches of $LiMgPO_4:Tb^{3+}$ phosphor (weight ~3 mg) under γ irradiation. The exposed pouches were kept in dark box. Each pouch was read for the different tenure in days. The experimental result was shown in figure 9, which shows that there was a loss of about 42% of the OSL signal within 10 days after which the intensity gets stabilized. This fading of the OSL signal may be thermal type and arises as the 150°C peak is of high amplitude.

Table 3. Kinetics parameters of $LiMgPO_4:Tb^{3+}$ in LM-OSL mode.

Phosphor	Component	ω/t_m	δ/t_m	τ/t_m	τ	δ	ω	μ_g
$LiMgPO_4:Tb^{3+}$	First	1.60	0.80	0.79	91	91	182	0.50
	Second	1.31	0.65	0.65	149	149	298	0.50
	Third	1.57	0.79	0.79	319	320	639	0.50

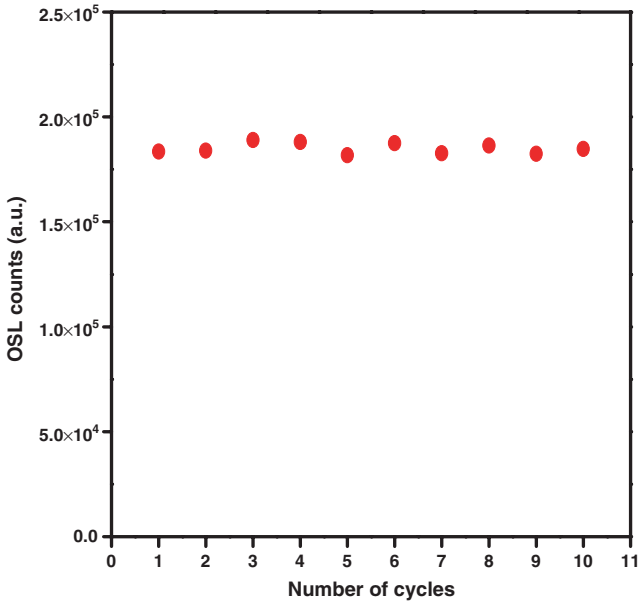

Figure 7. Reusability study of $LiMgPO_4:Tb^{3+}$ phosphor.

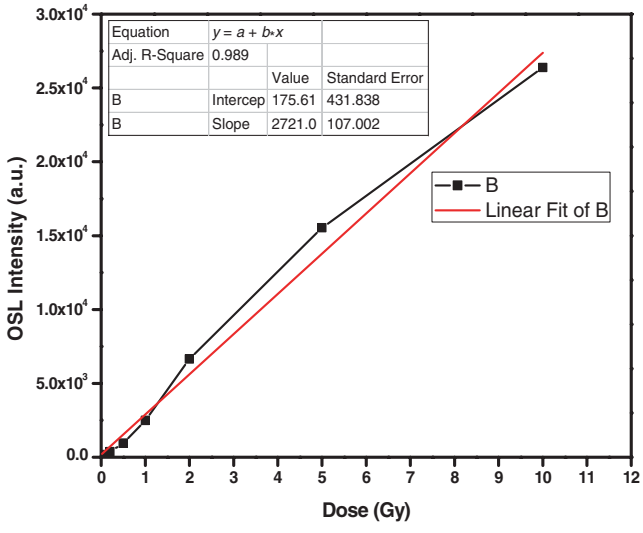

Figure 8. Dose response of $LiMgPO_4:Tb^{3+}$ phosphor.

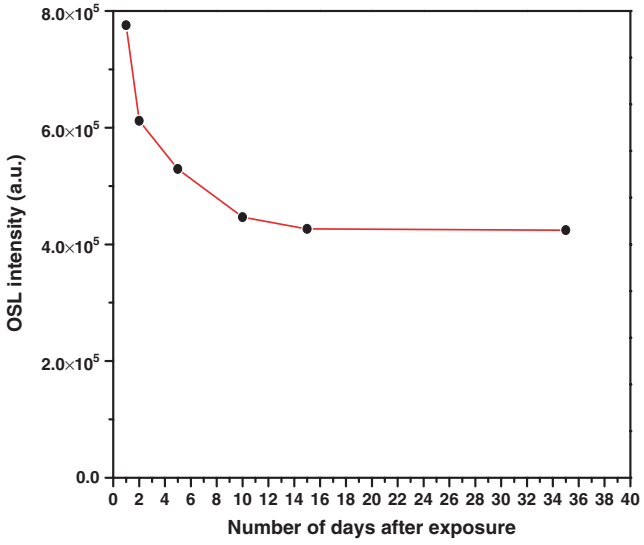

Figure 9. Fading response of $LiMgPO_4:Tb^{3+}$ phosphor.

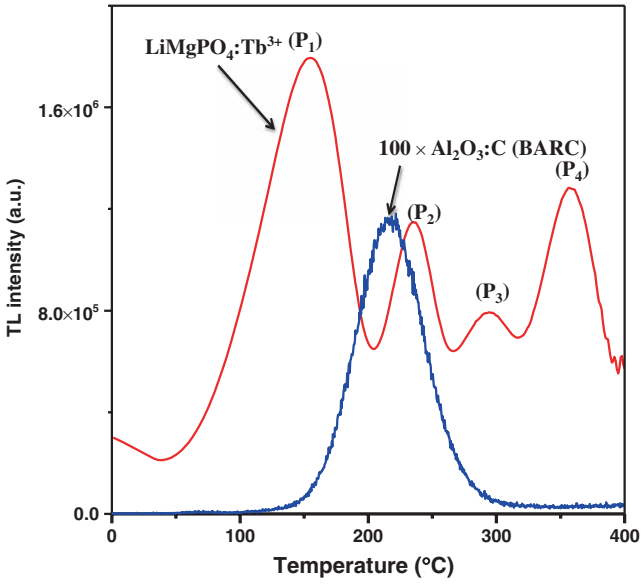

Figure 10. TL glow curve of $LiMgPO_4:Tb^{3+}$ phosphor compared with Al_2O_3:C (BARC) phosphor.

3.3h *TL characteristics*: Figure 10 shows the TL glow curves of $LiMgPO_4:Tb^{3+}$ phosphor under β irradiation (40 mGy). The TL glow curve of the $LiMgPO_4:Tb^{3+}$ phosphor consist overlapping peaks in temperature range of 25–400°C and first peak (P_1) was observed at 150°C, second peak (P_2) at 238°C, third peak (P_3) at 291°C and fourth peak (P_4) at 356°C. The TL sensitivity of second peak (P_2) of $LiMgPO_4:Tb^{3+}$ phosphor was compared with α-Al_2O_3:C (BARC) phosphor and found to be TL sensitivity of $LiMgPO_4:Tb^{3+}$ phosphor was 100 times that of the α-Al_2O_3:C (BARC) phosphor. For the comparison of TL sensitivity with other commercially available phosphors,

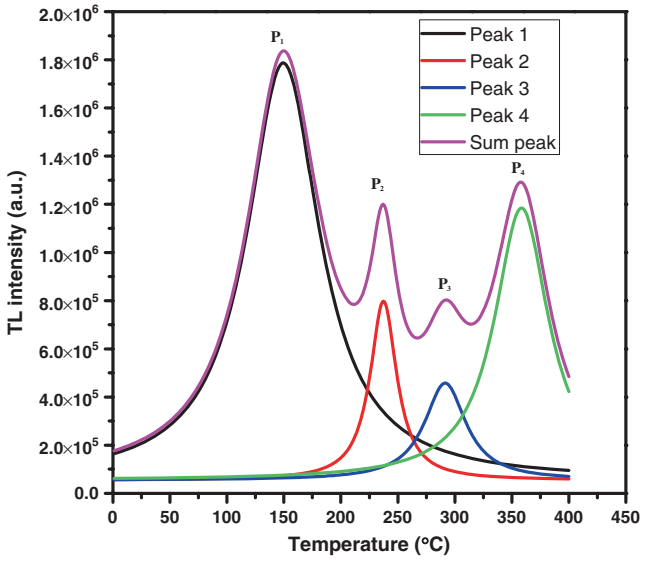

Figure 11. Deconvolution glow curve of $LiMgPO_4:Tb^{3+}$ phosphor.

Table 4. TL kinetic parameters of $LiMgPO_4:Tb^{3+}$ phosphor.

Measured TL parameters	$LiMgPO_4:Tb^{3+}$			
	150°C	238°C	291°C	356°C
E_m (eV)	0.616	2.474	1.801	1.876
s (s^{-1})	1.03×10^7	3.15×10^{24}	9.45×10^{15}	6.87×10^{15}
ω	79	31	51	61
δ	39	15	26	33
τ	40	16	25	28
μ_g	0.49	0.48	0.51	0.54
b	1.5	1.5	2	2

peak height of glow curve was used. However, the height of peak is proportional to the light intensity in a given temperature. Moreover, it is proportional to the mass of phosphor.

The study of kinetic parameters, such as activation energy (E_m), frequency factor(s) and order of kinetics (b) are considered an important part of TL. Actually TL glow curve composed of a number of overlapping peaks and these peaks are deconvoluted. Figure 11 shows the deconvoluted TL glow curve of $LiMgPO_4:Tb^{3+}$ phosphor. The kinetic parameters were calculated by using peak shape method [18,19] and calculated kinetic parameters were given in table 4.

3.3i *PL characteristics*: Excitation and emission spectra of $LiMgPO_4:Tb^{3+}$ phosphor was shown in figure 12. The excitation was measured at 544 nm and emission was measured at 224 nm. The excitation spectra consist of broad band around 224 nm, corresponds to 4f–5d transitions of Tb^{3+}. The emission spectrum consists of a series of sharp

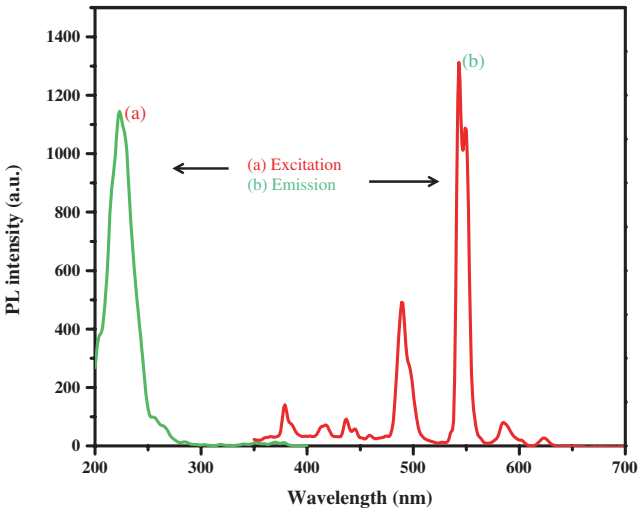

Figure 12. Excitation (**a**) and emission (**b**) spectra of $LiMgPO_4:Tb^{3+}$ phosphor.

lines peaking at 380, 418, 439, 490, 544, 583 and 621 nm corresponding to transitions $^5D_3$–$^7F_6$, $^5D_3$–$^7F_5$, $^5D_3$–$^7F_4$, $^5D_4$–$^7F_6$, $^5D_4$–$^7F_5$, $^5D_4$–$^7F_4$, $^5D_4$–$^7F_5$ and $^5D_4$–$^7F_6$, respectively [20].

4. Conclusions

In this work, $LiMg_{(1-x)}PO_4:xTb^{3+}$ ($x = 0.001, 0.002, 0.005, 0.01, 0.02$) phosphor was synthesized via modified solid state method. The OSL sensitivity of $LiMgPO_4:Tb^{3+}$ phosphor was 2.7 times that of $LiMgPO_4:Tb^{3+}$, B (BARC) and 4.3 times than that of α-Al_2O_3:C (BARC) phosphor. The TL sensitivity of second peak (P_2) of $LiMgPO_4:Tb^{3+}$ phosphor was 100 times than that of Al_2O_3:C (BARC) phosphor. The OSL components were determined by using CW-OSL and LM-OSL modes. The minimum detectable dose (MDD) was found to be 5.6 μGy with 3σ of background. Also, the reusability studies showed that the phosphor could be reused for 10 cycles without any change in the OSL output. The phosphor show linear dose response in OSL mode (0.04–10 Gy) and OSL signal was lost up to 42% at the end of 10 days, and after that the OSL intensity (signal) became constant. The $LiMgPO_4:Tb^{3+}$ phosphor is nearly tissue equivalent material and phosphor shows high sensitivity, linear dose response, better reusability, fading and MDD, this phosphor may be useful for radiation dosimetry applications. Also phosphor shows emission in NUV region when excited with 318 nm under UV source.

Acknowledgements

One of the authors CBP is very much thankful to Head, RPAD, Radiological Physics and Advisory Division, Bhabha Atomic Research Centre, Mumbai 400085, India, for providing the necessary facilities for the analysis of OSL and TL results.

References

[1] Gasparian P B R, Vanhavere F and Yukihara E G 2012 *Radiat. Meas.* **47** 243

[2] Yukihara E G and McKeever S W 2008 *Phys. Med. Biol.* **53** R351

[3] Huntley D J, Godfrey-Smith D I and Thewalt M L W 1985 *Nature* **313** 105

[4] Antonov-Romanovskii V, Keirum-Marcus I, Poroshina M and Trapeznikova Z 1955 USAEC Report AEC-tr-2435, Part 1239

[5] Lin C, Liu R, Tang Y and Hu S 2008 *J. Electrochem. Soc.* **155** J248

[6] Yang Z, Yang G, Wang S, Tian J, Li X, Guo Q and Fu G 2008 *Mater. Lett.* **62** 1884

[7] Yang R and Lai H 2014 *J. Lumin.* **145** 49

[8] Dhabekar B, Menon S, Alagu E, Bakshi A, Singh A, Chougaonkar M and Mayya Y 2011 *Nucl. Instrum. Methods Phys. Res. B* **269** 1844

[9] Gai M, Chen Z, Fan Y and Wang J 2013 *J. Rare Earths* **31** 551

[10] Palan C, Bajaj N, Soni A, Kulkarni M and Omanwar S 2015 *Bull. Mater. Sci.* **38** 1527

[11] More S, Meshram M, Wankhede S, Muthal P, Dhopte S and Moharil S 2011 *Phys. B* **406** 1178

[12] Palan C, Bajaj N, Soni A, Kulkarni M and Omanwar S 2016 *Rare Met.* DOI: 10.1007/s12598-015-0679-y

[13] Reddy J, Reddy J and Reddy J 2015 *Int. J. Lumin. Appl.* **5** 344

[14] Palan C, Bajaj N and Omanwar S 2016 *Mater. Res. Bull.* **76** 216

[15] Bulur E, Bùtter-Jensena L and Murray A S 2000 *Radiat Meas.* **32** 407

[16] Kumar M, Dhabekar B, Menon S, Chougaonkar M and Mayya Y 2011 *Nucl. Instrum. Methods Phys. Res., Sect. B* **269** 1849

[17] Rawat N, Dhabekar B, Kulkarni M, Muthe K, Mishra D, Soni A *et al* 2014 *Radiat. Meas.* **71** 212

[18] Bajaj N and Omanwar S 2012 *J. Rare Earths* **30** 1005

[19] Bajaj N and Omanwar 2014 *J. Lumin.* **148** 169

[20] Bajaj N, Palan C and Omanwar S 2015 *Int. J. Mat. Sci. Eng.* **3** 167